IEEE Access
Multidisciplinary | Rapid Review | Open Access Journal

Received September 25, 2018, accepted November 8, 2018, date of publication November 21, 2018,
date of current version December 27, 2018.

*Digital Object Identifier 10.1109/ACCESS.2018.2882527*

# Non-Destructive Identification of Weld-Boundary and Porosity Formation During Laser Transmission Welding by Using Optical Coherence Tomography

**KANGHAE KIM[1], PILUN KIM[2], JAEYUL LEE[1], SUWON KIM[2], SUNGJO PARK[3], SOO HO CHOI[3], JUNHO HWANG[3], JONG HOON LEE[3], (Member, IEEE), HO LEE[4], RUCHIRE ERANGA WIJESINGHE[5], MANSIK JEON[1], AND JEEHYUN KIM[1]**

[1]School of Electronics Engineering, College of IT Engineering, Kyungpook National University, Daegu 41566, South Korea
[2]Institute of Biomedical Engineering Research, Kyungpook National University, Daegu 41944, South Korea
[3]Laser Application Center, Institute of Advanced Convergence Technology, Kyungpook National University, Daegu 41061, South Korea
[4]School of Mechanical Engineering, Kyungpook National University, Daegu 41566, South Korea
[5]Department of Biomedical Engineering, Kyungil University, Gyeongsan 38428, South Korea

Corresponding authors: Ho Lee (jaeyul@knu.ac.kr), Ruchire Eranga Wijesinghe (eranga@kiu.kr), and Mansik Jeon (msjeon@knu.ac.kr)

This work was supported in part by the Industrial Key Technology Development Program through the Ministry of Trade, Industry and Energy, MI, South Korea, under Grant 10063360, in part by the Industrial Infrastructure Program of Laser Industry Support, which is through the Ministry of Trade, Industry & Energy, South Korea, under Grant N0000598, in part by the BK21 Plus Project though the Ministry of Education, South Korea, under Grant 21A20131600011, in part by the Bio & Medical Technology Development Program of the NRF through the Korean Government, MSIP, under Grant 2017M3A9E2065282, and in part by the National Research Foundation of Korea (NRF) Grant through the Korean Government, MSIT, under Grant 2018R1A5A1025137.

**ABSTRACT** Laser transmission welding offers significant benefits over conventional welding techniques enabling single-stage rapid plastic joining. The quality of laser transmission welded products is commonly assessed by measuring the weld penetration depth, hardened weld boundary, and inspecting the formation of porosity. However, the existing methods of verification are inevitably accompanied by destruction of the specimen. Thus, non-destructive quality assessment methods for laser transmission welding have gained attention recently. Here, we demonstrated an extended industrial application of 860 nm wavelength-based spectral domain optical coherence tomography for the non-destructive inspection of the aforementioned quality parameters of laser transmission welded industrial plastic materials, i.e., polycarbonate and acrylonitrile butadiene styrene copolymer. The acquired cross-sectional resolution and volumetric and intensity profiles sufficiently contributed to the quality assessment procedure, revealing the weld boundary and porosity formation, and thus confirming the potential applicability of optical coherence tomography for the quality inspection of laser transmission welded products.

**INDEX TERMS** Laser transmission welding, optical coherence tomography, polymers: thermoplastics.

## I. INTRODUCTION

Thermoplastic has been gradually replacing metals in the automotive, aerospace, and medical fabrication industries due to its advantages such as weight saving, flexibility, electrical and thermal insulation combined with electromagnetic interference shielding, and low cost [1]–[4]. Owing to the increased number of applications, numerous techniques have been employed for plastic welding including manual processes, vibration and frictional heating between materials, electromagnetic heat source based welding, and laser transmission welding [5]–[7]. Among them, laser transmission welding was first used in 1970 by employing CO2 laser [8], [9]. However, CO2 laser is not suitable for thermoplastic fabrication because it decomposes, vaporizes and carbonizes the structural surface before the heat is transmitted towards inside the structure and eventually deteriorates the internal material properties [10], [11]. The recent emergence of near infrared wavelength (NIR) Nd:YAG and diode lasers facilitated thermoplastic welding on the basis of selective transmission and absorption by using an appropriate filler [11]–[13]. Further, the advantages of this technology, including high quality welding seam, non-contact welding, and high bonding strength, led to its wide applications [14], [15]. This technique is particularly suitable for

medical applications owing to the small heat-affected zone that does not require any adhesives, which are harmful to the human body [4], [16].

The most commonly used methods for evaluating the properties of laser transmission welded products are visual inspection using optical micrographs, mechanical testing using lap-shear strength (LSS), and surface inspection using scanning electron microscopy. Air bubbles are generated during erroneous welding, which negatively affect the fatigue strength and airtightness. Inspection of the appearance of air bubbles is thus important to assess the quality of the welded products. However, optical microscopy and scanning electron microscopy can identify the air bubbles in the welded region approximately on the weld seam surface, but not exactly at the weld surface boundary. Thus, in order to inspect the cross-sectional properties, the welded specimen needs to be destructed [17], [18]. On the other hand, for normalized LSS measurement, accurate measurement of the welded interface is essential, which is mainly performed based on the area of the welded region. Although numerous studies were performed to examine LSS of diverse lap welds with various welding parameters [19]–[21], the difficulty of precise weld-area calculation degrades the accuracy of the LSS measurement. Moreover, the usage of conventional mechanical inspection techniques, such as displacement measurements and pyrometer based methods, have been limited due to the destructiveness, lack of quantitative information concerning the geometry of weld seam, and difficulty of inspecting different welded areas [17], [22]–[24]. Hence, the necessity for devising a non-destructive real-time inspection technique for laser transmission welding, which would provide information on the possible presence of imperfections formed during erroneous laser transmission welding, has gained remarkable attention.

Optical coherence tomography (OCT) is an optical medical imaging technique [25], [26], which was recently employed in diverse defect-inspection applications as a powerful inspection tool for industrial products owing to its high resolution (on the order of microns) and non-destructive imaging capability. Reinforced from the high axial and spatial resolution of OCT, numerous studies on defect inspection of paper, glass, liquid resins, and agricultural products by OCT have been reported in the literature [27]–[31]. In particular, OCT based quality assurance of laser transmission welded single-stage plastic was performed [18] to confirm the applicability of OCT for initial product inspection. Therefore, OCT can be considered as a potential solution for accurate localization and precise characterization of structural imperfections formed during laser transmission welding.

In the study proposed here, we demonstrated an OCT based initial quality assurance process for laser transmission welded materials to investigate the welded boundary and porosity formation. The primary focus of the study was to evaluate the inspection capability of OCT to identify structural perfections as well as imperfections formed during welding. The cross-sectional formation of stiffened bondage (during perfect welding) and the formation of porosities and air bubbles (during erroneous welding) between the utilized thermoplastic varieties, i.e., polycarbonate and acrylonitrile butadiene styrene copolymer, were evaluated using the acquired 2D OCT and 3D OCT images and intensity based A-scan depth profiles obtained from the OCT system. The main comparison and conceptual breakthrough of this study (compared to the study reported by Schmitt et.al.) is the utilization of high-resolution shorter wavelength range based economical SD-OCT system for the defect inspection of specific polycarbonate and acrylonitrile butadiene styrene copolymer material, where the longer wavelengths hardly visualized the deep regions of imperfectly welded region due to the materialistic properties. The results provided an elaborate comparison between successfully and unsuccessfully welded samples along with new insights into phenomena that occur during a imperfect welding process, which suggest that OCT holds a great potential for application in the laser transmission welding industry.

## II. MATERIALS AND METHODS

### A. LASER TRANSMISSION WELDDED SAMPLE

A high power pump laser system (YLR-500, IPG, USA) with a wavelength of 1070 nm was used for laser transmission welding. The applied laser intensity for welding was 50 W. Although welding is possible at an intensity of 5 W, here we used maximum configurable intensity of the laser system (50 W) to obtain a perfect weld region as the primary goal of the study well as to obtain the imperfect weld region, which was the secondary experimental purpose. Therefore, the laser dosimetry was applied while considering the material degradation through calculated the temperature-time data of the point located at the maximum temperature. The laser beam was collimated and irradiated on the sample with a beam size of 6 mm. The welding speed of the laser was 50 mm/s, and it took approximately 2 s for a complete weld. Figure 1(a) shows a representative schematic diagram of the laser transmission welding system used for joining two thermoplastic materials. The two different materials used for welding are: a laser-transparent material (polycarbonate with the 99% transmittance) and a laser-absorbing material (acrylonitrile butadiene styrene copolymer). The aforementioned materials were selected with similar dimensions (20 cm $\times$ 5 cm) except for their thickness. The thickness of polycarbonate was 3 mm and that of acrylonitrile butadiene styrene copolymer was 4.5 mm. The polycarbonate layer was placed on top of the acrylonitrile butadiene styrene copolymer layer and the laser beam was transmitted to weld the two layers together. To minimize gap formation between the two materials during the welding process, the two materials were clamped on either side. The indicated regions of interest (ROI 1 and 2) in Fig. 1(b), 1(c), and 1(d) emphasize the regions investigated using OCT after the welding process. Fig. 1(b) shows a pictorial representation of the laser transmission welded thermoplastic materials along with the microscopically (100$\times$) magnified ROI 1 and 2. The gray

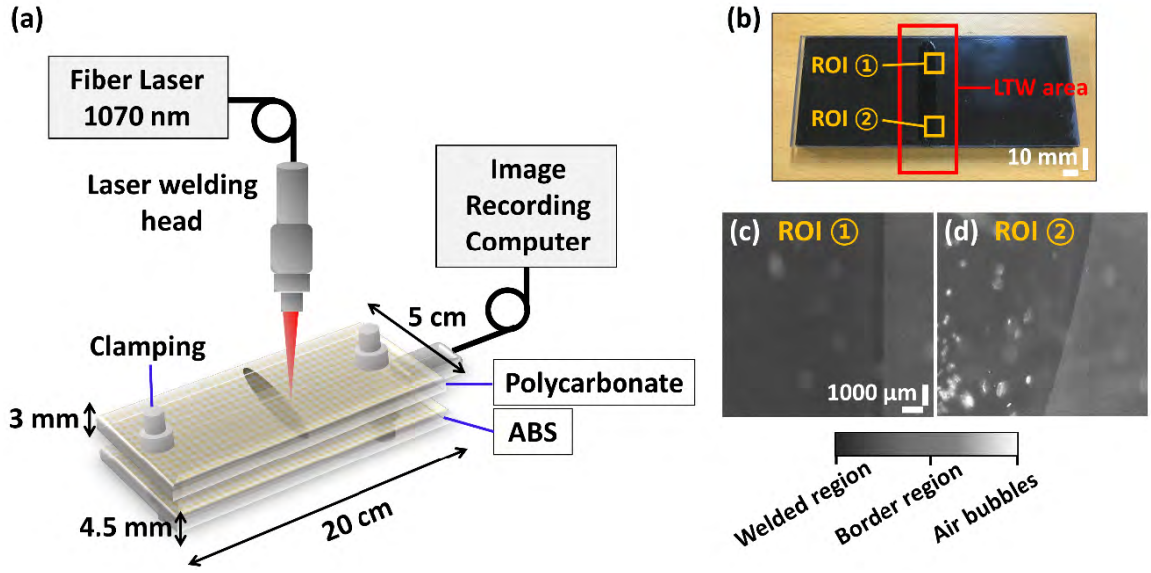


**FIGURE 1.** (a) Schematic of the used laser transmission welding process. (b) Graphical representation of welded thermoplastic materials. (c), (d) Grayscale representation of the microscopically 100X magnified inspected regions of interest (ROI 1 and 2). The abbreviations: ABS: acrylonitrile butadiene styrene copolymer, LTW: laser transmission welding.

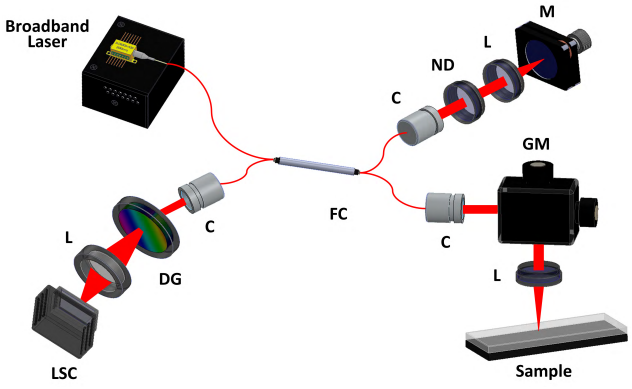


**FIGURE 2.** Schematic of the SD-OCT system. The abbreviations: C: collimator, DG: diffraction grating, FC: fiber coupler, GM: galvano mirror, L: lens, LSC: line scan camera, M: mirror, ND: neutral density filter.

scale images in Fig. 1(c) and (d) provide an illustration of the different regions (perfectly welded, imperfectly welded, and border regions). Since, the primary focus of the study was to investigate the potential applicability of the corresponding wavelength range based OCT system, and therefore the quality inspection of a particular specimen consists of polycarbonate and acrylonitrile butadiene styrene copolymer materials was involved.

### B. SD-OCT SYSTEM

Figure 2 shows the schematic of the employed 840-nm SD-OCT system in the study. The light source of the OCT is a broadband laser (EXS210022-01, Exalos Ltd., Swiss) centered at $\lambda$ c = 840 nm with a full width at half maximum (FWHM) of 50 nm. The output beam of broadband laser is passed towards the sample arm and reference arm through a 50:50 fiber coupler (FC850-40-50-APC, Thorlabs, Inc., USA). The reference arm consists of a collimator (FC850-40-50-APC, Thorlabs, Inc., USA), a lens (AC254-030-B, Thorlabs, Inc., USA), and a mirror (ME1-G01, Thorlabs, Inc., USA). A neutral density filter (NDC-50C-2M-B, Thorlabs, Inc., USA) was used for control the intensity. The sample arm consists of a collimator (FC850-40-50-APC, Thorlabs, Inc., USA), a galvanometer scanner (GVS002; Thorlabs, Inc., USA), and a lens (AC254-030-B, Thorlabs, Inc., USA). The collimated beam is scanned in the transverse direction using a galvanometer scanner and focused using an objective lens with a focal length of 30 mm. The length of the scanned ROI was 5 mm. The inverse scattering light from the sample arm and that from the reference arm are combined and delivered to the spectrometer through an optical coupler. The interference signal was connected to the spectrometer, which consists of a collimator (F810APC-842, Thorlabs, Inc., USA), a transmission-type diffraction grating (spatial frequency 1800 lpmm, Wasatch Photonics, USA) with nominal diffraction angle of 46.05°, lens(AC508-100-B; Thorlabs, Inc., Newton, NJ, USA), and a line scan camera (spL4096-140 km, Basler, Germany). The measured axial resolution of the system is 8 $\mu$m, and the lateral resolution is 13 $\mu$m. The signal-to-noise ratio of the spectrometer was measured as 101 dB. Eight hundred A-scans were used to create real-time 2D OCT images. Each A-scan has a depth of 4.7 mm in the depth direction. We used 1000 images to create a 3D OCT image. The scan range for creating 3D OCT images is 5 mm × 5 mm. The system acquired a 2D OCT image at 40 frames/s and took 25 s to acquire a single image of a 3D image.

## III. RESULTS AND DISCUSSION

### A. OCT EVALUATION OF PERFECTLY WELDED REGION

Figure 3(a) shows the cross-sectionally analyzed OCT image of the perfectly welded region, which is indicated in the

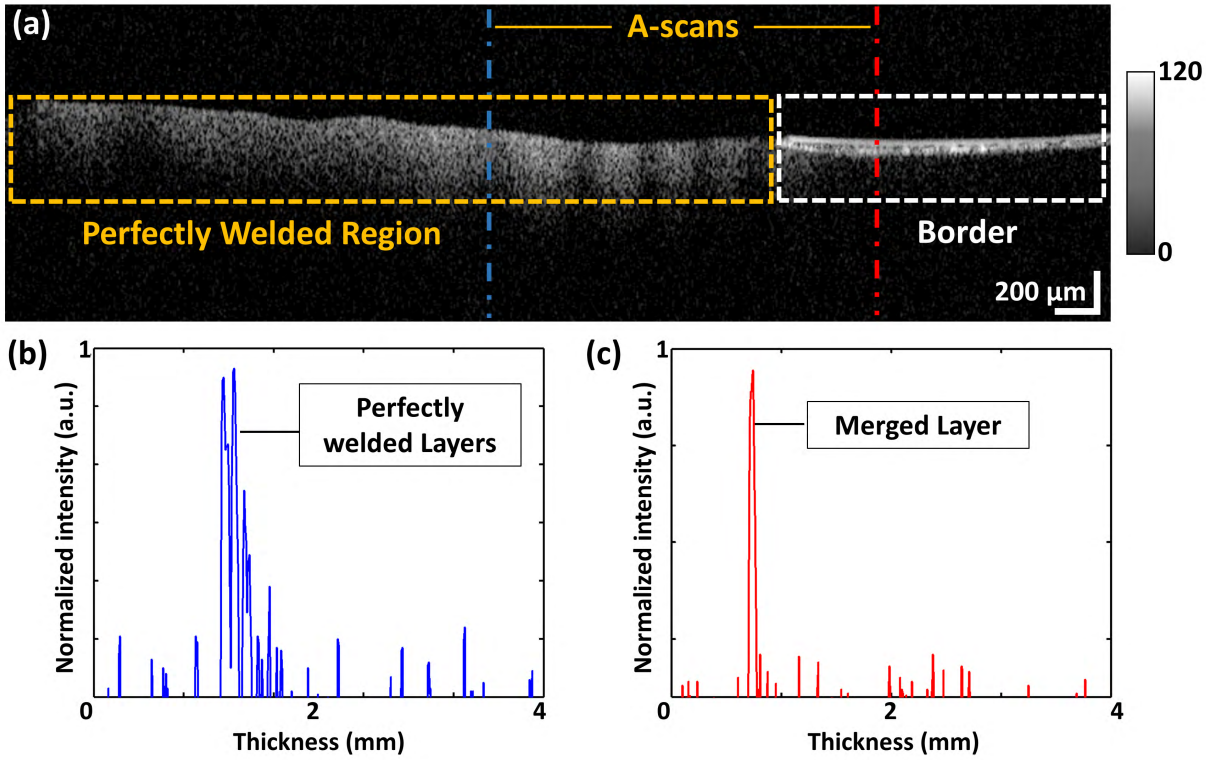


**FIGURE 3.** 2D OCT representation and depth direction intensity profile (A-scan) evaluations for a perfectly laser transmission welded region. (a) 2D OCT image of the perfectly welded sample. (b), and (c) are the A-scan plots of the welded and non-welded border regions. The broad orange dashed box is the welded region, and the narrow white dashed box is the non-welded border region. The blue and red dot-dashed lines indicated on the OCT image correspond to the plotted region of (b) and (c) A-scan profiles, respectively. The gray-scale intensity conversion from the logarithmic OCT images are scaled from 0 ∼ 120.

ROI 1 of Fig. 1(c). The broad orange dashed box indicates the region, where the welding was performed and the narrow white dashed box indicates the boundary of the welded region. It was visually confirmed that the weld seam width and the intersection between the laser-transparent material and the laser-absorbing material disappears due to the melting of laser-transparent polycarbonate. Although the structural change can be visually identified, information is limited to the topographical range. Nevertheless, the cross-sectional representation of Fig. 3(a) reveals the presence and the absence of layer information in depth direction more precisely in both welded and border regions. A clear difference between the two regions can be visualized owing to the change of refractive index in the perfectly welded region, followed by the melted region. The preciseness of the thickness information can be enhanced by calculating the refractive index for each region, which requires further technical aspects. Therefore based on the fundamental OCT conditions, 1.58, which is the refractive index of polycarbonate and acrylonitrile butadiene styrene copolymer materials was simply utilized for both quantitative and qualitative measurements, where the measurements were later normalized for transparency. Consequently, in the border region, layer thickness information of the top joining partner (polycarbonate) can be identified with a different cross-sectional view from the welded region. To enhance the accuracy of the qualitative representations, depth direction intensity profiling was performed for the acquired 2D OCT images. Figures 3(b) and (c) are the depth direction intensity profiles obtained from the welded and non-welded regions corresponding to the blue and red dot-dashed lines indicated in Fig. 3(a). The depth direction intensity A-scan profiles provide a clear correlation to the cross-sections exhibiting quantitative thickness information, such as 300 $\mu$m in the welded region, and 100 $\mu$m in the non-welded boundary region of particular layers. OCT images and A-scan plots were used to identify differences in thickness and intensity in the welded region and non-welded regions on the materials, thereby distinguishing between the welded regions and non-welded regions. As illustrated in the results, the depth direction intensity depth profiles acquired from the corresponding images exploit the depth dependent thickness detection capability of the OCT method, which will be a potential aid for the industrial utility.

### *B. OCT EVALUATION OF IMPERFECTLY WELDED REGION*

To gain a sufficient understanding of the potential applicability of OCT under various circumstances, the welding time of the ROI 2 shown in Fig. 1(d) were exceeded compared to ROI 1. Fig. 4(b) is the cross-sectionally analyzed

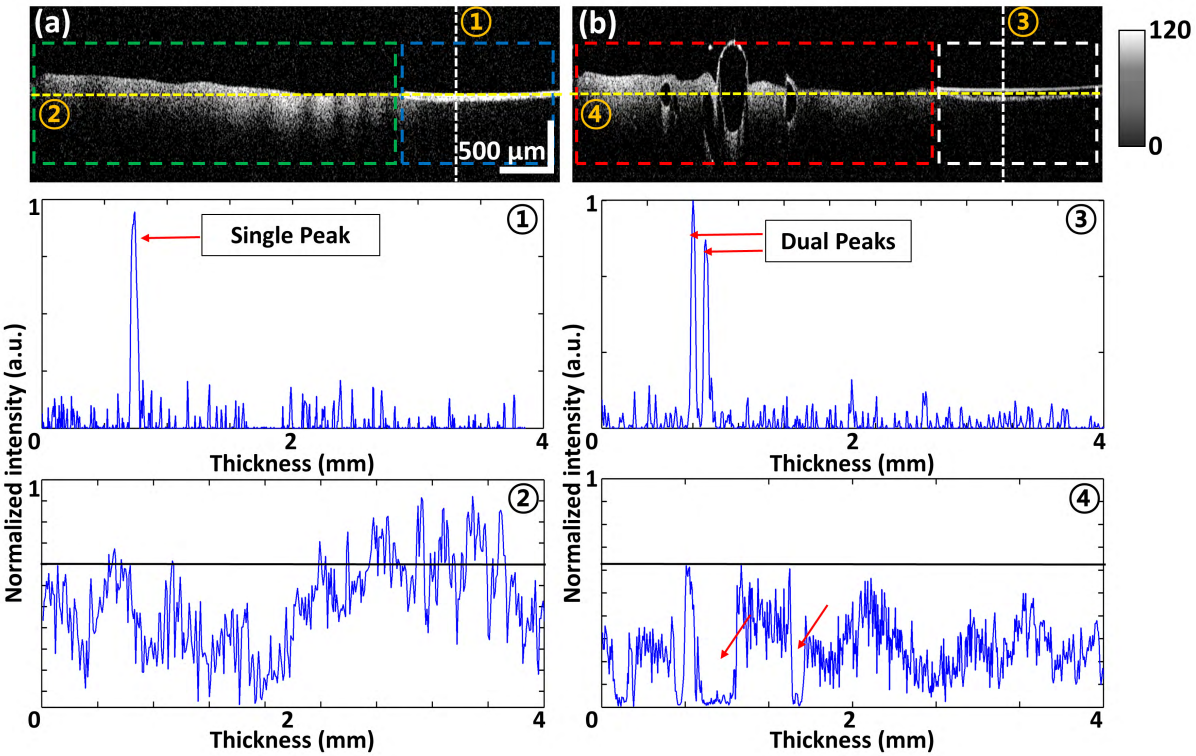


**FIGURE 4.** Qualitative and quantitative comparison between the perfectly and the imperfectly laser-transmission-welded regions. (a) 2D OCT image of a perfectly welded sample. (b) 2D OCT image of the imperfectly welded sample. The white color vertical dashed lines shown on 4(a) and 4(b) numbered with No.1 and No.3 defines the exact locations of axial direction A-scan intensity profiles and corresponding graphical results are numbered with No.1 (4c) and No.3 4(d) plots. The yellow color horizontal dashed lines shown on 4(a) and 4(b) numbered with No.2 and No.4 defines the exact locations of lateral direction A-scan intensity profiles and corresponding graphical results are numbered with No.2 (4e) and No.4 (4f) plots.

OCT image of the imperfectly welded joint partner regions. The green and blue dashed boxes of Fig. 4(a) is a cross-sectional 2D OCT image of a perfectly welded region, and the red and white dashed boxes represent the cross-sections of the imperfectly welded regions. Both Fig. 4(a) and (b) was obtained on the coronal plane of the sample. As shown in Fig. 4(b), the OCT images acquired from imperfectly welded regions characterize the formation of porosities and air bubbles in the weld seam revealing the defectiveness of the laser transmission welding process. In addition to the aforementioned cross-sectional changes, a distinct gap formation (different from section 3.1) in the non-welded (boundary) region was significantly characterized owing to the depth penetration and high resolution of OCT. In addition, it was confirmed that the gap is formed at the junction of the laser-transparent material and the laser-absorbing material in the non-welded boundary region as shown in Fig. 4(b). Similar axial depth intensity evaluation was performed here for the imperfectly welded region using A-scans to analyze the intensity fluctuations. Besides axial intensity analysis, structural changes and porosity formation of both welded regions were characterized. The white dashed lines in the axial direction indicated along with the numbers 1 and 3 in Fig. 4(a) and (b) correspond to the exact position in which the axial direction intensity was evaluated. The yellow dashed lines in the lateral direction indicated along with the numbers 2 and 4 in Fig. 4(a) and (b) correspond to the exact position in which the lateral direction intensity was evaluated. A well-distinguishable single peak correlating the border of a perfectly welded sample is shown in plot No.1. A clear verification of the distinct gap formation in the border of a imperfectly welded sample is illustrated in plot No.2. The lateral direction intensity fluctuation provides a comparison of intensity peaks between the two regions (ROI 1 and 2). As the structural property differences, such as the presence of melted region and porosities, exist in the OCT tomograms, the fluctuation of intensity peaks clearly correlate to the tomograms as shown in plots No.3 and No.4 of Fig. 4. In addition, the formation of air bubbles and gaps lead to a reduction of pixel intensity in tomograms shown in Fig. 4(b) compared to 4(a). Thus, a reduction of the intensity level in Fig. 4(b) compared to 4(a) can be identified in No.2 and No.4 lateral direction intensity profiles. Moreover, the red arrows in No.4 exhibit the intensity correlation to the aforestated porosities. Since, the quality of laser transmission welded products are commonly assessed by destructively measuring the weld penetration depth, hardened weld boundary, and inspecting the formation of porosity, the acquired qualitative cross-sectional information and the quantitative depth profile results acquired using OCT system clearly revealed the information weld penetration depth as a measure of inspecting the welds.

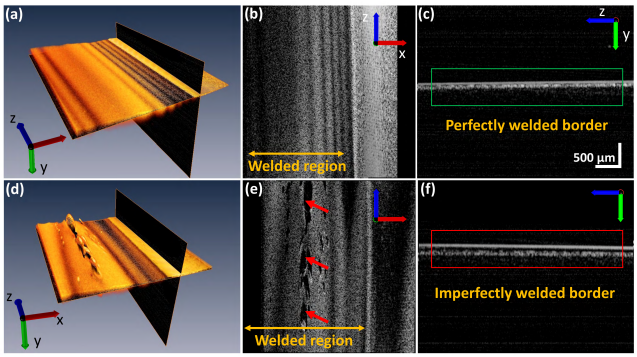


**FIGURE 5.** 3D volumetric OCT representation of welded sample. (a) 3D OCT image of perfectly welded sample. (b) Corresponding enface OCT image and (c) structural formation in an additional orthogonal plane. (d) 3D OCT image of imperfectly welded sample. (e) Corresponding enface OCT image, and (f) structural formation in an additional orthogonal plane.

### C. THREE-DIMENSIONAL OCT EVALUAION OF PERFECTLY AND IMPERFECTLY WELDED REGION

The three-dimensionally (3D) analyzed depth-direction enface OCT images well below the top surface are illustrated in Fig. 5. The acquired 3D OCT images were prepared by combining 900 tomograms into 3D data array and then rendered. The 3D OCT images were rendered with commercial or open-source software particularly designed for this purpose. The perfectly welded region (5a) and imperfectly welded region (5b) were three-dimensionally analyzed. The orthosliced enface images acquired from the y-direction orthogonal plane of each Fig 5(a) and 5(d) are emphasized in Figure. 5(b) and 5(e). Further, the orthosliced enface images acquired from the x-direction orthogonal plane of each Fig 5(a) and 5(d) are emphasized in Figure. 5(c) and 5(f). Although the obtained tomograms enabled us to identify the formation and localize the porosities, the rendered 3D OCT images exhibit vital information confirming the distribution of porosities, air bubbles, and perfectly welded regions, which is useful in quality assessments. Moreover, the aforementioned gap formation between the two layers during imperfect welding can be precisely visualized in the enface image acquired from the orthogonal plane in x- direction. Hence, these multi-direction inspection factors of OCT technology immensely contribute to the thermoplastic welding industry, as the quality of thermoplastic joints based on the perfect and imperfect welding can be evaluated in a rapid and non-destructive manner in real-time, which makes our method superior to the existing inspection techniques.

## IV. CONCLUSION

The utilization of micrometer resolution of OCT for the industrial defect inspection is a conceptual breakthrough. Hence, the aim of this study was to exploit the potential merits of OCT by qualitatively and quantitatively evaluating the formation of defects including porosities and air bubbles during laser transmission welding in a non-destructive manner. The precisely obtained results clearly revealed the anticipated advantages of OCT by providing a precise cross-sectional and three-dimensional visualizations of perfectly welded regions, imperfectly welded regions, and porosity formations internally. Moreover, we were able to distinguish the structural differences between the welded and the non-welded regions during laser transmission welding through the assessment of depth direction intensity (A-scan) profiles of OCT images, which provided a robust quality assessment compared to conventional techniques. As an additional benefit of OCT, the acquired 2D, 3D, and enface images can be utilized to a great extent in future studies to obtain an accurate numerical expression for the weld area calculations, which is an essential requirement for the LSS techniques. Therefore, with the escalation of laser-transmission-welding-based thermoplastic fabrications and applications in recent micro and nanotechnology, OCT will play a vital role by serving as a defect-inspecting quality assurance method with a high sensitivity rendering the technique as an essential tool in industry.

## ACKNOWLDEGMENT

Kanghae Kim and Pilun Kim contributed equally to this work.

## REFERENCES

[1] A. Yousefpour, M. Hojjati, and J.-P. Immarigeon, "Fusion bonding/welding of thermoplastic composites," *J. Thermoplastic Compos. Mater.*, vol. 17, pp. 303–341, Jul. 2004.

[2] J. M. P. Coelho, M. A. Abreu, and F. C. Rodrigues, "Modeling $CO_2$ laser radiation transmission lap welding of thermoplastic films: Energy balance approximation," *Opt. Eng.*, vol. 46, no. 6, p. 064301, 2007.

[3] A. Benatar and T. G. Gutowski, "Method for fusion bonding thermoplastic composites," *SAMPE Q, United States*, vol. 18, no. 1, pp. 329–330, 1986.

[4] N. Amanat, N. L. James, and D. R. McKenzie, "Welding methods for joining thermoplastic polymers for the hermetic enclosure of medical devices," *Med. Eng. Phys.*, vol. 32, pp. 690–699, Sep. 2010.

[5] R. J. Wise, *Thermal Welding of Polymers*. Cambridge, U.K.: Woodhead Publishing, 1999.

[6] R. Rudolf, P. Mitschang, M. Neitzel, and C. Rueckert, "Welding of high-performance thermoplastic composites," *Polym. Polym. Compos.*, vol. 7, no. 5, pp. 309–315, 1999.

[7] D. M. Maguire, "Joining thermoplastic composites," *SAMPE J.*, vol. 25, no. 1, pp. 11–14, 1989.

[8] H. Silvers, Jr., and S. Wachtell, "Perforating, welding and cutting plastic films with a continuous $CO_2$ laser," Penn State College Eng., University Park, PA, USA, Tech. Rep., 1970, pp. 88–97.

[9] C. Rüffler and K. Gürs, "Cutting and welding using a $CO_2$ laser," *Opt. Laser Technol.*, vol. 4, pp. 265–269, Dec. 1972.

[10] M. J. Cieslak and P. W. Fuerschbach, "On the weldability, composition, and hardness of pulsed and continuous Nd:YAG laser welds in aluminum alloys 6061,5456, and 5086," *Metall. Trans. B*, vol. 19, no. 2, pp. 319–329, 1988.

[11] P. A. Hilton, I. Jones, and Y. Kennish, "Transmission laser welding of plastics," in *Proc. 1st Int. Symp. High-Power Laser Macroprocessing*, 2003, pp. 44–53.

[12] V. A. Kagan, R. G. Bray, and W. P. Kuhn, "Laser transmission welding of semi-crystalline thermoplastics—Part I: Optical characterization of nylon based plastics," *J. Reinforced Plastics Compos.*, vol. 21, no. 12, pp. 1101–1122, 2002.

[13] V. A. Kagan and G. P. Pinho, "Laser transmission welding of semicrystalline thermoplastics—Part II: Analysis of mechanical performance of welded nylon," *J. Reinforced Plastics Compos.*, vol. 23, pp. 95–107, Jan. 2004.

[14] H. Herfurth, "New approaches in plastic welding with diode lasers," in *Proc. 18th Int. Congr. Appl. Lasers Electro-Optics*, San Diego, CA, USA, 1999.

[15] I. Jones, "Use of infrared dyes for transmission laser welding of plastics," in *Proc. ICALEO*, Nov. 1999.

[16] Y. Miyashita, T. Watanabe, and Y. Otsuka, "Formation behavior of bubbles and its effect on joining strength in dissimilar materials laser spot joining between PET and SUS304," *Mech. Eng. J.*, vol. 2, no. 1, pp. 429-1–429-14, 2015.
[17] N. Amanat, C. Chaminade, J. Grace, D. R. McKenzie, and N. L. James, "Transmission laser welding of amorphous and semi-crystalline polyether–ether–ketone for applications in the medical device industry," *Mater. Des.*, vol. 31, pp. 4823–4830, Dec. 2010.
[18] R. Schmitt, G. Mallmann, M. Devrient, and M. Schmidt, "3D polymer weld seam characterization based on optical coherence tomography for laser transmission welding applications," *Phys. Procedia*, vol. 56, no. 2014, pp. 1305–1314, 2014.
[19] Y. S. Sato, A. Shiota, H. Kokawa, K. Okamoto, Q. Yang, and C. Kim, "Effect of interfacial microstructure on lap shear strength of friction stir spot weld of aluminium alloy to magnesium alloy," *Sci. Technol. Weld. Joining*, vol. 15, no. 4, pp. 319–324, 2010.
[20] L. F. M. da Silva, T. N. S. S. Rodrigues, M. A. V. Figueiredo, M. F. S. F. de Moura, and J. A. G. Chousal, "Effect of adhesive type and thickness on the lap shear strength," *J. Adhes.*, vol. 82, no. 11, pp. 1091–1115, 2006.
[21] S. H. Chowdhury, D. L. Chen, S. D. Bhole, X. Cao, and P. Wanjara, "Lap shear strength and fatigue behavior of friction stir spot welded dissimilar magnesium-to-aluminum joints with adhesive," *Mater. Sci. Eng. A*, vol. 562, pp. 53–60, Feb. 2013.
[22] T. Ussing, L. V. Petersen, C. B. Nielsen, B. Helbo, and L. Højslet, "Micro laser welding of polymer microstructures using low power laser diodes," *Int. J. Adv. Manuf. Technol.*, vol. 33, pp. 198–205, May 2007.
[23] G. Newaz, T. Sultana, S. Nusier, and H. J. Herfurth, "Miniaturized samples for bond strength and hermetic sealing evaluation for transmission laser joints," *J. Laser Micro/Nanoeng.*, vol. 3, no. 3, pp. 186–195, 2008.
[24] J. Stavridis, A. Papacharalampopoulos, and P. Stavropoulos, "Quality assessment in laser welding: A critical review," *Int. J. Adv. Manuf. Technol.*, vol. 94, pp. 1825–1847, Feb. 2018.
[25] D. Huang *et al.*, "Optical coherence tomography," *Science*, vol. 254, no. 5035, pp. 1178–1181, 1991.
[26] W. Jung, J. Kim, M. Jeon, E. J. Chaney, C. N. Stewart, and S. A. Boppart, "Handheld optical coherence tomography scanner for primary care diagnostics," *IEEE Trans. Biomed. Eng.*, vol. 58, no. 3, pp. 741–744, Mar. 2011.
[27] M.-T. Tsai, F.-Y. Chang, Y.-C. Yao, J. Mei, and Y.-J. Lee, "Optical inspection of solar cells using phase-sensitive optical coherence tomography," *Sol. Energy Mater. Solar Cells*, vol. 136, pp. 193–199, May 2015.
[28] Z. Chen, Y. Shen, W. Bao, P. Li, X. Wang, and Z. Ding, "Identification of surface defects on glass by parallel spectral domain optical coherence tomography," *Opt. Express*, vol. 23, no. 18, pp. 23634–23646, 2015.
[29] T. Prykäri, J. Czajkowski, E. Alarousu, and R. Myllylä, "Optical coherence tomography as an accurate inspection and quality evaluation technique in paper industry," *Opt. Rev.*, vol. 17, no. 3, pp. 218–222, 2010.
[30] R. E. Wijesinghe, K. Park, Y. Jung, P. Kim, M. Jeon, and J. Kim, "Industrial resin inspection for display production using automated fluid-inspection based on multimodal optical detection techniques," *Opt. Lasers Eng.*, vol. 96, pp. 75–82, Sep. 2017.
[31] R. E. Wijesinghe *et al.*, "Optical coherence tomography-integrated, wearable (backpack-type), compact diagnostic imaging modality for *in situ* leaf quality assessment," *Appl. Opt.*, vol. 56, no. 9, pp. D108–D114, 2017.

**KANGHAE KIM** is currently pursuing the Ph.D. degree with the School of Electronics Engineering, Kyungpook National University, Daegu, South Korea. His research background includes optical imaging techniques, optical coherence tomography, endoscopic systems of the optical coherence tomography, and photoacoustic tomography.

**PILUN KIM** received the Ph.D. degree from the Department of Medical and Biological Engineering, Kyoungpook National University, in 2011. He is currently a Researching Visiting Professor with the Institute of Biomedical Engineering, Kyungpook National University. He is interested in translating new technologies from the research field to the application field, such as clinic and industrial and making its productization. His main interests are biomedical device development, optical coherence tomography, and digital image processing.

**JAEYUL LEE** is currently pursuing the Ph.D. degree with the School of Electronics Engineering, Kyungpook National University, Daegu, South Korea. His research background includes optical imaging techniques, photoacoustic microscopy, optical coherence tomography, and handheld instruments for optimization of the optical coherence tomography and photoacoustic microscopy system.

**SUWON KIM** is currently pursuing the Ph.D. degree with the School of Electronics Engineering, Kyungpook National University, Daegu, South Korea. His research background includes laser processing techniques, hetero-juction, welding, and micro fabricating.

**SUNGJO PARK** received the Ph.D. degree in electronics engineering from Kyungpook National University, Daegu, South Korea, in 2015. He was a Research Assistant Professor with the Department of Creative IT Engineering, POSTECH. He is currently a Principal Researcher with the Laser Application Center, Kyungpook National University. His research interests are in the development of nonionizing and noninvasive novel biomedical imaging techniques, including photoacoustic tomography, photoacoustic microscopy, optical coherence tomography, and other novel applications of laser processing.

**SOO HO CHOI** was born in 1980. He received the B.S. degree from the Department of Mechanical Engineering, Kumoh National Institute of Technology, Gumi, Gyeongbuk, South Korea, in 2006. He is currently pursuing the M.S. degree in mechanics with Kyungpook National University (KNU). He worked at Mirae thermotec Cooperation as a Process Control Engineer and DiC Cooperation as a Manufacturing Engineer from 2006 to 2013. He spent one and half years at Daegu Mechatronics & Materials Institutes as a Senior Researcher. Since 2015, he has been with the Laser Application Center, KNU. His major interest is laser machining.

**JUNHO HWANG** is currently pursuing the Ph.D. degree with the Department of Dental Science, Graduate School, Kyungpook National University, Daegu, South Korea. His research interests are the development of material and manufacturing processes for 3D printing application and high power laser processing, including additive manufacturing, laser welding, and laser hardening.

**JONG HOON LEE** (M'11) was born in 1975. He received the M.S. and Ph.D. degrees from the School of Electrical Engineering and Computer Science, Kyungpook National University (KNU), Daegu, South Korea, in 2000 and 2007, respectively. He joined the Photonic Network Research Lab, KAIST, as a Post-Doctoral Researcher in 2007. He worked at the Electronics and Telecommunications Research Institute, from 2009 to 2011, as a Senior Researcher. Since 2012, he has been a Research Professor with the Laser Application Center, KNU. His major interests include laser material processing and biophotoic techniques.

**HO LEE** received the Ph.D. degree in mechanical engineering from The University of Texas at Austin, USA, in 2003. He was a Research Fellow with the Wellman Institute of Photomedicine, Harvard Medical School. He is currently a Professor with Kyungpook National University, Daegu, South Korea. His research interest is in laser machining and biomedical imaging.

**RUCHIRE ERANGA WIJESINGHE** received the B.Sc. and Ph.D. degrees in electronics engineering from Kyungpook National University, Daegu, South Korea, in 2012 and 2018, respectively. He is currently an Assistant Professor with the Department of Biomedical Engineering, Kyungil University. His research interests are in the development of high-resolution novel biological and biomedical imaging techniques including optical coherence tomography and microscopy for clinical utility.

**MANSIK JEON** received the Ph.D. degree in electronics engineering from Kyungpook National University, Daegu, South Korea, in 2011. He is currently as an Assistant Professor with the School of Electronics Engineering, Kyungpook National University. His research interests are in the development of nonionizing and noninvasive novel biomedical imaging techniques, including photoacoustic tomography, photoacoustic microscopy, optical coherence tomography, ultrasonic imaging, handheld scanner, and their clinical applications.

**JEEHYUN KIM** received the Ph.D. degree in biomedical engineering from The University of Texas at Austin, USA, in 2004. He was a Post-Doctoral Researcher with the Beckman Laser Institute, University of California at Irvine. He is currently a Full Professor with Kyungpook National University, Daegu, South Korea. His research interest is in biomedical imaging and sensing, neuroscience studies using multiphoton microscopy, photo-acoustic imaging, and other novel applications of sensors.